CHEMISTRY OF
MATERIALS
Article

*Chem. Mater.* **2009,** *21,* 5319–5326
DOI:10.1021/cm902506a

# Applications of Photocurable PMMS Thiol−Ene Stamps in Soft Lithography

Luis M. Campos,[†] Tu T. Truong,[‡] Dong Eun Shim,[§] Michael D. Dimitriou,[†]
Daniel Shir,[‡] Ines Meinel,[∥] Jeffrey A. Gerbec,[∥] H. Thomas Hahn,[§]
John A. Rogers,[‡] and Craig J. Hawker*[,†]

[†]*Materials Research Laboratory, Mitsubishi Chemical Center for Advanced Materials, Department of Chemistry and Biochemistry, and Materials Department, University of California, Santa Barbara, California 93106,* [‡]*Department of Chemistry, Department of Materials Science and Engineering, and Department of Electrical and Computer Engineering, Beckman Institute and Frederick Seitz Materials Research Laboratory, University of Illinois at Urbana-Champaign, Urbana, Illinois 61801,* [§]*Department of Mechanical and Aerospace Engineering and Multifunctional Composites Laboratory, University of California, Los Angeles, California 90095, and* [∥]*MC Research and Innovation Center, 601 Pine Avenue, Goleta, California 93117*

*Received August 14, 2009. Revised Manuscript Received September 28, 2009*

We report the performance and characterization of a material based on poly[(3-mercaptopropyl)-methylsiloxane] (PMMS) in various soft lithography applications. PMMS stamps were made by cross-linking with triallyl cyanurate and ethoxylated (4) bisphenol A dimethacrylate via thiol−ene mixed-mode chemistry. The surface chemistry of the materials was characterized by XPS when varied from hydrophilic through oxygen plasma treatment, to hydrophobic by exposure to a fluorinated trichlorosilane agent. The materials are transparent above 300 nm and thermally stable up to 225 °C, thus rendering them capable to be employed in step-and-flash imprint lithography, nanoimprint lithography, nanotransfer printing, and proximity-field nanopatterning. The successful pattern replication from the micrometer to sub-100 nm scale was demonstrated.

## Introduction

Nanoimprinting techniques continue to attract considerable interest because of their potential to enable mass production of nanopatterns and nanostructures at low cost and submicrometer resolution.[1,2] Traditional nanoimprint lithography (NIL), developed by Chou and co-workers,[3] takes advantage of the moldable characteristics of polymer melts by heating a polymer film above its glass transition temperature ($T_g$), while being pressed with a topographically patterned hard master. Upon cooling, the thermoplastic polymer maintains the inverse structure of the master. With this technology, the mold is generally a hard material, such as a silicon wafer or a metal to prevent any deformation of the patterned features during the imprint process. As an alternative to traditional NIL, step and flash imprint lithography (SFIL) was developed by Willson and co-workers.[4] SFIL utilizes UV light to cure a thin film photoresist while being pressed with the patterned master, thus allowing the imprinting step to be done in the absence of high temperatures. Another major advantage provided by this technique is the ability to optically align the master with the template to control the spatial location of imprinted patterns. However, a patterned quartz master is necessary to allow UV light to penetrate the master and cure the photoresist. To avoid the complications that arise from using hard, specialty masters (such as quartz), soft lithography emerged as a low-cost, high throughput alternative that takes advantage of a single master to fabricate myriad disposable polymeric replicas.[5,6] To further enable this technology, we have recently introduced a new family of inexpensive, cross-linkable soft materials capable of replicating high fidelity sub-100 nm features with curing times of 1−2 min.[7] In this manuscript we report the use of these systems in traditional soft lithographic applications, and we characterize the physical properties that are relevant for the viability of these processes.

Soft lithography involves the fabrication of an inverse replica of a patterned hard master using cross-linkable polymeric materials.[8,9] Generally, a liquid mixture of

---

*Corresponding author. E-mail: hawker@mrl.ucsb.edu.

(1) Menard, E.; Meitl, M. A.; Sun, Y.; Park, J. U.; Shir, D. J. L.; Nam, Y. S.; Jeon, S.; Rogers, J. A. *Chem. Rev.* **2007**, *107*, 1117–1160.
(2) del Campo, A.; Arzt, E. *Chem. Rev.* **2008**, *108*, 911–945.
(3) Chou, S. Y.; Krauss, P. R.; Renstrom, P. J. *Science* **1996**, *272*, 85–87.
(4) Colburn, M.; Johnson, S. C.; Stewart, M. D.; Damle, S.; Bailey, T. C.; Choi, B.; Wedlake, M.; Michaelson, T. B.; Sreenivasan, S. V.; Ekerdt, J. G.; Willson, C. G. *Proc. SPIE* **1999**, *3676*, 379–389.
(5) Xia, Y.; Kim, E.; Zhao, X.-M.; Rogers, J. A.; Prentiss, M.; Whitesides, G. M. *Science* **1996**, *273*, 347–349.
(6) Xia, Y.; Whitesides, G. M. *Angew. Chem., Int. Ed.* **1998**, *37*, 550–575.
(7) Campos, L. M.; Meinel, I.; Guino, R. G.; Schierhorn, M.; Gupta, N.; Stucky, G. D.; Hawker, C. J. *Adv. Mater.* **2008**, *20*, 3728–3733.
(8) Xia, Y.; Rogers, J. A.; Paul, K. E.; Whitesides, G. M. *Chem. Rev.* **1999**, *99*, 1823–1848.
(9) Gates, B. D.; Xu, Q.; Stewart, M.; Ryan, D.; Willson, C. G.; Whitesides, G. M. *Chem. Rev.* **2005**, *105*, 1171–1196.

small molecules and polymers is cast onto the patterned master and cured. The cross-linked polymeric stamp is then peeled and further used in a wide variety of soft lithography processes,[1] such as soft nanoimprint lithography, soft step and flash lithography, and nanotransfer pritinting, among others.[10] This technique allows for the fabrication of multiple, inexpensive stamps from a single hard master. While several polymeric materials have been developed,[11−13] employing various types of cross-linking chemistries, the most widely used are based on the platinum catalyzed hydrosilylation of poly(dimethylsiloxane) (PDMS). These systems are generally cured by heating but require extended periods of time, prohibiting high throughput fabrication. Although fast-curing systems have been developed,[14−16] they suffer from one or more of the following: (a) oxygen inhibition during cross-linking, (b) high-cost materials, and (c) the use of specialized equipment to replicate sub-100 nm features.

To avoid the above complications, materials based on poly[(3-mercaptopropyl)methylsiloxane] (PMMS) have been developed for applications in soft lithography.[7] PMMS can be cured via thiol−ene click chemistry with a wide array of alkene-containing cross-linkers.[17] The modularity imparted by these versatile systems allows for high throughput stamp fabrication and optimization of the resulting physical, chemical, and mechanical properties.[18] Furthermore, the rapid curing and molding of the materials via thiol−ene click chemistry can be done at ambient conditions,[19] without inhibition from oxygen or moisture,[20] by simply casting the prepolymer liquid mixture onto the patterned masters. Given the nature of the curing chemistry, having control over the cross-linking of the systems allows the liquid mixture to fully infiltrate the master molds, thus yielding high fidelity features.

To study the pattern transfer capabilities of the PMMS-based systems, we have selected the mixture composed of PMMS, triallyl cyanurate (TAC), and ethoxylated (4) bisphenol A dimethacrylate (BPADMA, Scheme 1). The resulting cross-linked material has an elastic modulus, *E*, of approximately 24 MPa (elongation at break ca. 20%), and the films (ca. 0.5 mm thick) are stiffer than the commercially available PDMS (Sylgard 184, *E* of ca. 2−3 MPa) but are also flexible, rendering them useful in SNIL. This material has been successfully used to pattern photonic crystals of titania[21] and micrometer arrays via microcontact printing.[22]

**Scheme 1**

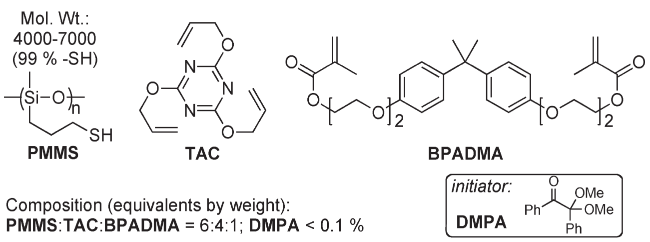

## Results and Discussion

**Stamp Fabrication Process.** One of the most beneficial aspects of the PMMS materials is the ease of processing to fabricate patterned stamps (Figure 1). As previously described, the process involves the thorough mixing of PMMS, TAC, and BPADMA, along with less than 0.1 wt % of the UV-active radical initiator DMPA (this mixture is referred to as sample blend 2, or SB2). The liquid SB2 is then cast between an ordinary microscope glass slide and a patterned silicon master using Teflon spacers to control the thickness of the stamps (ca. 0.5 mm). It is preferred to treat the masters with the fluorinating agent (tridecafluoro-1,1,2,2-tetrahydrooctyl)trichlorosilane ($Cl_3SiCH_2CH_2[CF_2]_5CF_3$, TDFOCS) by vapor deposition to enhance the release properties of the stamps. The mixture is then cured using UV light (365 nm) at ambient conditions (without previous deoxygenation) for 2 min (Figure 1B). Finally, the stamp is released by peeling from the master (Figure 1C). We must note that no pressure is required to fill the master mold in Figure 1B.[16]

**Physical Properties.** To be able to use the materials in SSFIL, the stamp must be transparent to the light required to cure photoresists.[4,23] Figure 2 shows the percent transmittance spectra of the cross-linked blend. The material is optically clear and transparent above 300 nm (ca. 90% transmission at 350 nm). We must note that using too much radical initiator (DMPA) can lead to absorbance at wavelengths between 300 and 400 nm, which arise from the $n,\pi^*$ transition from DMPA (see Figure 2, inset). As a result, the acetophenone initiator should be added to the blends in quantities less than 0.1 wt % to achieve the transmittance displayed in Figure 2, or other initiators, such as AIBN (thermally active), can also be employed to avoid the absorbance

---

(10) Moran, I. W.; Cheng, D. F.; Jhaveri, S. B.; Carter, K. R. *Soft Matter* **2008**, *4*, 168–176.

(11) (a) Truong, T. T.; Lin, R.; Jeon, S.; Lee, H. H.; Maria, J.; Gaur, A.; Hua, F.; Meinel, I.; Rogers, J. A. *Langmuir* **2007**, *23*, 2898–2905. (b) Choi, K. M.; Rogers, J. A. *J. Am. Chem. Soc.* **2003**, *125*, 4060.

(12) Khan, A.; Malkoch, M.; Montague, M. F.; Hawker, C. J. *J. Polym. Sci., Polym. Chem.* **2008**, *46*, 6238–6254.

(13) Rolland, J. P.; Hagberg, E. C.; Denison, G. M.; Carter, K. R.; DeSimone, J. M. *Angew. Chem., Int. Ed.* **2004**, *43*, 5796.

(14) Choi, K. M. *J. Phys. Chem. B* **2005**, *109*, 21525–21531.

(15) Rolland, J. P.; Maynor, B. W.; Euliss, L. E.; Exner, A. E.; Denison, G. M.; DeSimone, J. M. *J. Am. Chem. Soc.* **2005**, *127*, 10096–10100.

(16) Pina-Hernandez, C.; Kim, J. S.; Guo, L. J.; Fu, P. F. *Adv. Mater.* **2007**, *19*, 1222–1227.

(17) Hoyle, C. E.; Lee, T. Y.; Roper, T. *J. Polym. Sci., Part A: Polym. Chem.* **2004**, *42*, 5301–5338.

(18) Hagberg, E. C.; Malkoch, M.; Ling, Y.; Hawker, C. J.; Carter, K. R. *Nano Lett.* **2007**, *7*, 233–237.

(19) (a) Killops, K. L.; Campos, L. M.; Hawker, C. J. *J. Am. Chem. Soc.* **2008**, *130*, 5062–5064. (b) Campos, L. M.; Killops, K. L.; Sakai, R.; Paulusse, J. M. J.; Damiron, D.; Drockenmuller, E.; Messmore, B. W.; Hawker, C. J. *Macromolecules* **2008**, *41*, 7063–7070.

(20) (a) Johnson, P. M.; Stansbury, J. W.; Bowman, C. N. *J. Polym. Sci., Part A: Polym. Chem.* **2008**, *46*, 1502–1509. (b) Nilsson, C.; Simpson, N.; Malkoch, M.; Johansson, M.; Malmström, E. *J. Polym. Sci., Part A: Polym. Chem.* **2008**, *46*, 1339–1348.

(21) Truong, T. A.; Campos, L. M.; Matioli, E.; Meinel, I.; Hawker, C. J.; Weisbuch, C.; Petroff, P. M. *Appl. Phys. Lett.* **2009**, *94*, 023101.

(22) von Werne, T. A.; Germack, D. S.; Hagberg, E. C.; Sheares, V. V.; Hawker, C. J.; Carter, K. R. *J. Am. Chem. Soc.* **2009**, *125*, 3831–3838.

(23) Long, B. K.; Keitz, B. K.; Willson, C. G. *J. Mater. Chem.* **2007**, *17*, 3575–3580.

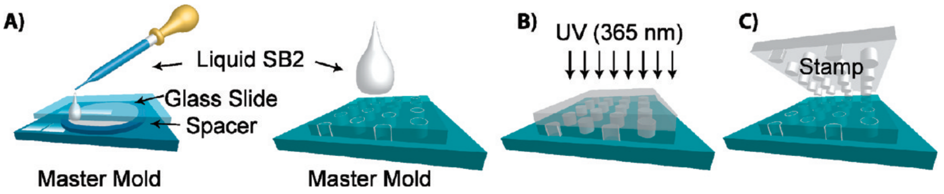

**Figure 1.** Process for stamp fabrication: (A) Cast liquid SB2 onto a patterned master mold. (B) Cure the material with UV light for 2 min at ambient conditions. (C) Peel the patterned polymeric stamp.

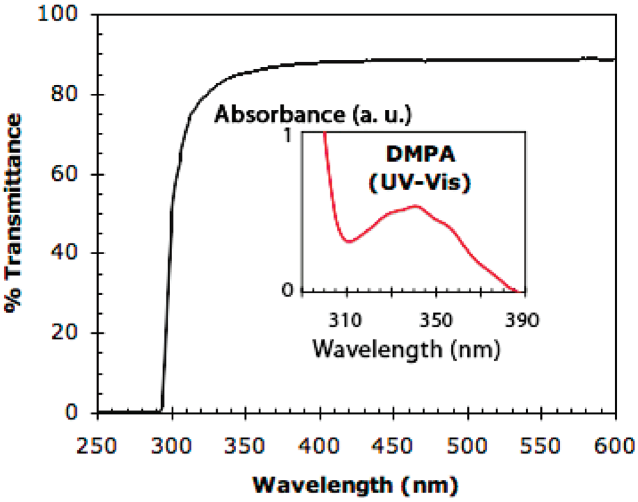

**Figure 2.** Percent transmittance spectrum of a 0.5 mm thick film of SB2. The inset shows the UV−vis spectrum of DMPA in chloroform, highlighting the n → $\pi^*$ transition between 310 and 380 nm.

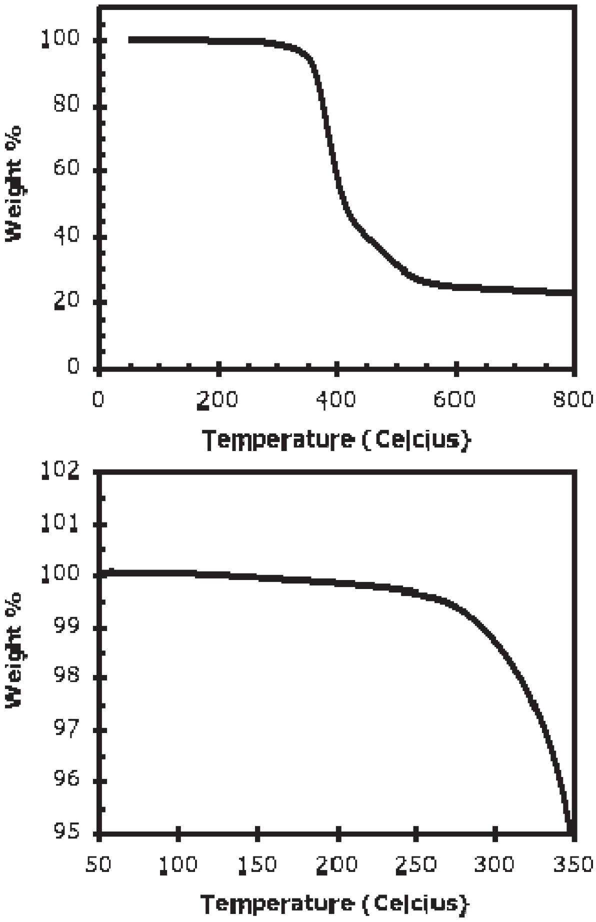

**Figure 3.** Top: Complete profile of the thermogravimetric analysis (TGA) of SB2 (heating rate of 10 °C/min). Bottom: Expanded region of the TGA plot.

from the 310−390 nm UV-active initiator. The PMMS-based material (SB2) is comparable to *s*-PDMS and *h*-PDMS, which are transparent to light above 300 nm.[11] The newly modified, acrylate-functional perfluoropolyether stamps (a-PFPE, an extension of the work developed by DeSimone and co-workers)[13] reported are transparent above approximately 350 nm (40% transmission at 350 nm, 2 mm thick films).[11]

With the potential to use the PMMS materials to transfer patterns using moldable thermoplastics (such as embossing),[3,24] both thermogravimetric analysis (TGA, Figure 3) and differential scanning calorimetry (DSC) were carried out to obtain information regarding the thermal stability of SB2. The TGA plot shows that decomposition begins to take place near 250 °C (Figure 3, bottom), a value comparable to that of Sylgard 184.[25] Above 300 °C, the SB2 rapidly decomposes due to the high organic content from the alkene cross-linkers. Furthermore, within the temperature range from −80 to 220 °C, SB2 does not undergo any phase transitions as observed by DSC (within the lower temperature limit of the instrument). The result is analogous to Sylgard 184, which has a glass transition temperature ($T_g$) of approximately −120 °C.[26] The thermal stability of the PMMS material renders it with the capability to thermally cure or emboss materials at temperatures up to approximately 225 °C.

**Soft Step and Flash Imprint Lithography** (SSFIL)**.** The process for SSFIL is highlighted in Figure 4, where a soft stamp is used to press the moldable liquid photoresist.[10,11] While applying pressure, the photoresist is then cured to maintain the inverse pattern of the stamp. For any nanoimprint process, it is important that the resist does not adhere to the mold after imprinting.[23] To test the capability of SB2 to print the photoresist NXR-2010, the SSFIL procedure was carried out by applying pressure followed by UV light exposure (365 nm) for 1 min. As it is clearly visible from the optical microscope image in Figure 5A, the photoresist adhered to the SB2 stamp, and the pattern was ripped during the peeling process (Figure 4C).

---

(24) King, E.; Xia, Y.; Zhao, X.-M.; Whitesides, G. M. *Adv. Mater.* **1997**, *9*, 651–654.
(25) Johnson, R. T., Jr.; Biefeld, R. M.; Sayre, J. A. *Polym. Eng. Sci.* **1984**, *24*, 435–441.
(26) Lahiff, E.; Leahy, R.; Coleman, J. N.; Blau, W. J. *Carbon* **2006**, *44*, 1525–1529.

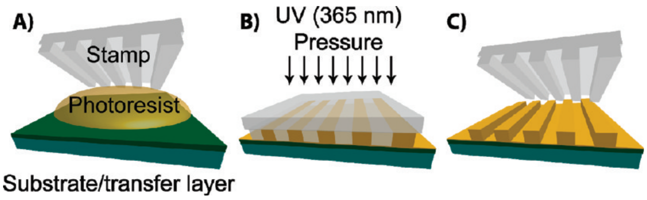

**Figure 4.** Process for pattern transfer via SSFIL: (A) Cast/spin coat liquid photoresist onto substrate with or without transfer layer. (B) Apply pressure and cure with UV light ($\lambda$ > 300 nm using SB2-F). (C) Peel the patterned polymeric stamp.

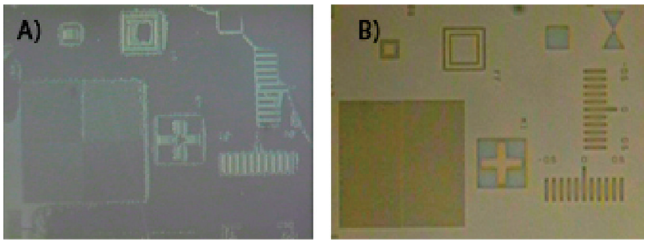

**Figure 5.** Microscope images of the patterns imprinted using two different stamps (50×). (A) Pristine stamp, without the surface treatment shows significant adherence. (B) Stamp with the hydrophobic surface treatment.

Given that PDMS materials can be modified at the surface to become hydrophilic by exposure to oxygen plasma,[27] the same treatment was applied to SB to oxidize the surface and subsequently functionalize with the same fluorinating agent that was used for the silicon masters and other PDMS stamps, TDFOCS.[10] To characterize the surface treatment, a nonpatterned, 2 mm thick film of SB2 was exposed to $O_2$ plasma for 15 s (300 mbar, 0.1 V). Longer exposure times have been shown to yield a silica layer in PDMS, which has been exploited as an impermeable layer to avoid deformations during SSFIL.[10] However, for the purpose of this work, 15 s was enough to change the water contact angle to < 17°, as opposed to the original value of 75°. A similar oxidation process was employed by Donzel et al. to make the surface of PDMS hydrophilic after 30 s of $O_2$ plasma treatment.[27] After exposing the surface to TDFOCS vapor under line vacuum for 20 min in an enclosed chamber, the water contact angle changed from < 17° to 103°, rendering it hydrophobic, in agreement with the similar treatment of PDMS.[10]

The surface treatment process for SB was also characterized by X-ray photoelectron spectroscopy (XPS). This technique allowed for the identification of the elements present at the surface before (SB2) and after exposure to $O_2$ plasma (SB2-OH) and after surface functionalization with TDFOCS (SB2-F). Figure 6 shows the evolution of the spectra at each step. From the composition of the blend, SB2 shows the expected presence of C, N, O, S, and Si. After $O_2$ plasma, the intensity of the O 1s peak noticeably increased in SB2-OH, relative to the C 1s peak. Finally, the incorporation of the covalently bound TDFOCS is evident by the appearance of the F 1s peak at approximately 690 eV. These steps are in accord with the observations by XPS in a similar treatment of PDMS.[10,27]

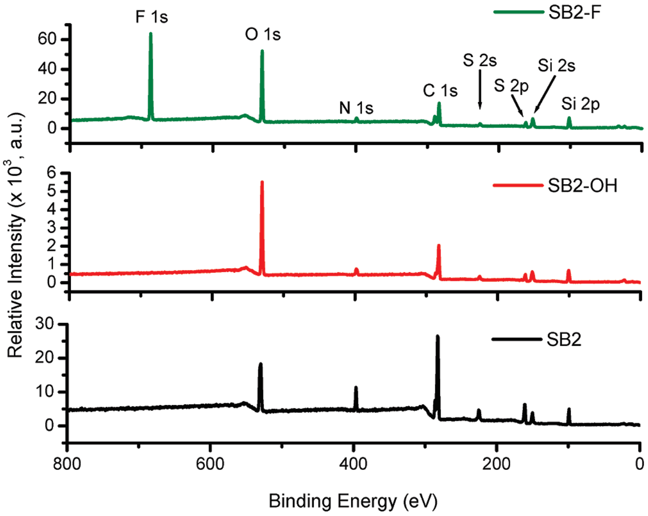

**Figure 6.** XPS spectra showing the elemental composition at the surface of SB2 (bottom), SB2-OH (center), and SB2-F (top).

Following the procedure depicted in Figure 7 to coat the fluorinating agent, TDFOCS, onto the surface of the polymeric stamp, SB2-F was implemented in the SSFIL process to pattern the photoresist NXR-2010. Under the same conditions described earlier, the processes proved to be successful and allowed peeling of the stamp from the printed substrate. Minimal adhesion was experienced when peeling the stamp, and the microscope image in Figure 5B does not show any imperfections.

The composition chosen (SB2) has various advantages over hard, patterned substrates, such as flexibility, low cost, and ease of fabrication. In SSFIL/SNIL, a flexible mold can conform to surfaces during the imprint step, thus significantly reducing defects caused by particles or dust trapped between the mold and the substrate. Given that pressure is applied to transfer the patterns, the mechanical properties of the materials are critical in SNIL.[11] Soft materials that have a low Young's modulus, such as PDMS, have critical drawbacks for their implementation in imprint lithography, and it is widely known that pressure can lead to collapse of the features.[28]

To test submicrometer pattern transfer to the NXR-2010 photoresist under pressure and illumination, the fluorinated SB2-F stamp in Figure 8A was employed as shown in Figure 4 and exposed to UV light through the top side of the stamp with the transparency of the PMMS material allowing for the curing of the photoresist (365 nm). The process involved applying pressure and illumination of the photoresist for 1 min. After the printing step, the stamp was peeled with minimal adhesion to the substrate. To improve adhesion of the resist to the substrate, the silicon wafer was pretreated with 3-(trimethoxysilane)propyloxyacrylate by solution deposition. The patterned stamp in Figure 8A contains features of posts with a height of approximately 200 nm, width

---

(27) Donzel, C.; Geissler, M.; Bernard, A.; Wolf, H.; Michel, B.; Hilborn, J.; Delamarche, E. *Adv. Mater.* **2001**, *13*, 1164–1167.

(28) Hui, C. Y.; Jagota, A.; Lin, Y. Y.; Kramer, E. J. *Langmuir* **2002**, *18*, 1394–1407.

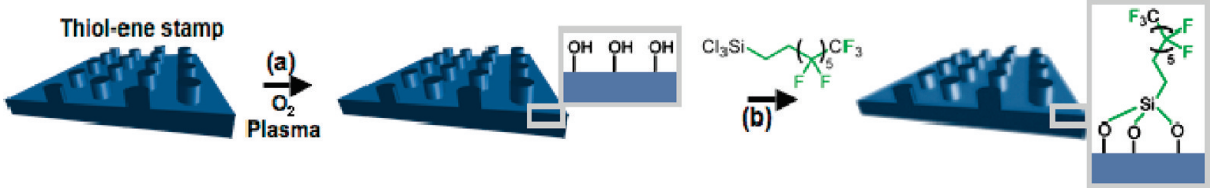

**Figure 7.** Process for coating SB2 with a fluorinated release layer: (A) expose SB2 to $O_2$ plasma for 15 s (yields SB2-OH) and (B) exposure of the hydrophilic stamp to TDFOCS vapor under vacuum for 20 min (yields SB2-F). See Figure 6 for the corresponding XPS surface analysis.

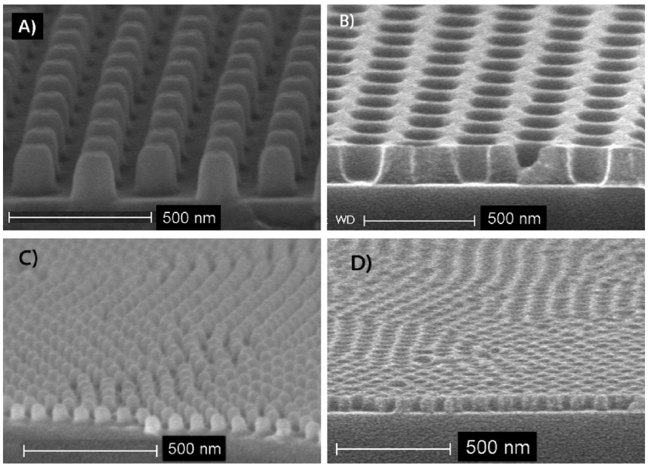

**Figure 8.** SEM images of (A) SB2-F stamp with 180 nm features and (B) the patterned photoresist NXR-2010 on silicon using the stamp in Figure 8A (film thickness ca. 200 nm, pores ca. 180 nm wide) and (C) SB2-F stamp with 55 nm features and (D) the patterned photoresist on Si (film thickness ca. 80 nm, pores ca. 60 nm wide).

approximately 170 nm, and period approximately 250 nm. The SEM image of the printed photoresist in Figure 8B shows the remarkably well-replicated inverse structure of the stamp. Furthermore, the patterning of sub-100 nm pores was accomplished using an SB2-F stamp fabricated using a porous aluminum oxide (PAO) master to yield posts as previously reported.[7] Figure 8C shows the SEM image of the printed photoresist (thickness ca. 70 nm, pore width ca. 55 nm). In both cases there are no apparent imperfections of the posts arising from the applied pressure. Another challenge in SFIL is the production of a scum layer with a key feature of PFPE-based systems being the ability to print resists without a scum layer,[11,15] that is, a residual layer of resist that prevents the surface exposure at the bottom of the pores/wells of the patterned substrates. Using the SB2-F stamps, the cross-sectional SEM images of the printed photoresist clearly shows no observable scum layer at the bottom of the wells, a preeminent feature of PFPE stamps.[11,15] Thus, the PMMS materials display outstanding characteristics, which show promise for replacing the hard masters traditionally employed in SSFIL.

**Soft NanoImprint Lithography (SNIL).** To test the printing capabilities of a thermoplastic resist, the commercially available NXR-1020 was used. This material can be spin coated onto a substrate, heated above its $T_g$, and molded by applying pressure. The printing process is highlighted in Figure 9 using SB2-F. However, this process requires high temperatures and higher pressures than those used in SSFIL, exposing the soft materials to harsh conditions and rendering the relief features prone to collapse.[28] Thus, the SB2-F stamps were subjected to the SNIL process using the pattern of posts shown in Figure 8A. The substrate preparation, without a transfer layer, involved the spin coating of a thin layer of the thermoplastic resist by spin coating on a clean silicon substrate. Using a Nanonex Imprinter (NX 2000), the stamp/NXR-1020/substrate sandwich shown in Figure 9 was subjected to 400 psi of pressure and 140 °C for 1 min. Upon immediate cooling, the stamp was peeled with minimal adhesion, and the transferred pattern was characterized by SEM.

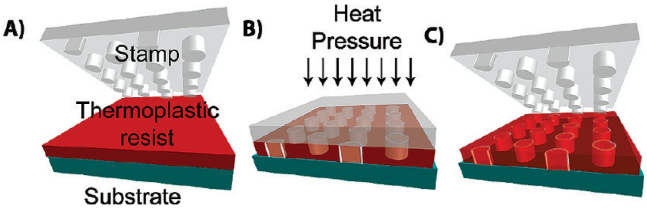

**Figure 9.** Process for pattern transfer via SNIL: (A) Spin coat the thermoplastic resist solution onto a substrate and allow to dry the film under vacuum at 50 °C for 2 h. (B) Apply pressure (400 psi) and heat (140 °C) for 1 min (using SB2-F as the stamp). (C) Peel the patterned polymeric stamp.

The SEM image of the patterned SB2-F stamp, composed of posts, is shown in Figure 8A, and the inverse features transferred onto the thermoplastic resist NXR-1020 are shown in Figure 10A. The resulting pattern has holes that are slightly wider than the posts of the stamp (width ca. 190 nm), but the depth is similar to the height of the posts (ca. 200 nm). This may be due to possible distortions arising from the pressure exerted during the printing process. However, the posts did not collapse under the severe conditions of the process, and the polymeric stamp could be used multiple times. It was also noticed that a residual scum layer of approximately 18 nm remained after the imprint process, which is common when patterning thermoplastic resists.[29,30] The scum layer was easily removed by conventional dry etching procedures. After exposing the patterned thermoplastic resist to $O_2$ plasma for 30 s, the scum layer is completely removed, exposing the surface of the silicon wafer. Further exposure to $O_2$ plasma for a total time of 60 s leads to widening of the pores (width ca. 240 nm), further exposing the surface of the substrate. Under the same conditions, the thermoplastic resist was embossed using

---

(29) Kim, S.; Lee, J.; Jeon, S.-M.; Lee, H. H.; Char, K.; Sohn, B.-H. *Macromolecules* **2008**, *41*, 3401–3404.

(30) Dumond, J.; Low, H. Y. *Adv. Mater.* **2008**, *20*, 1291–1297.

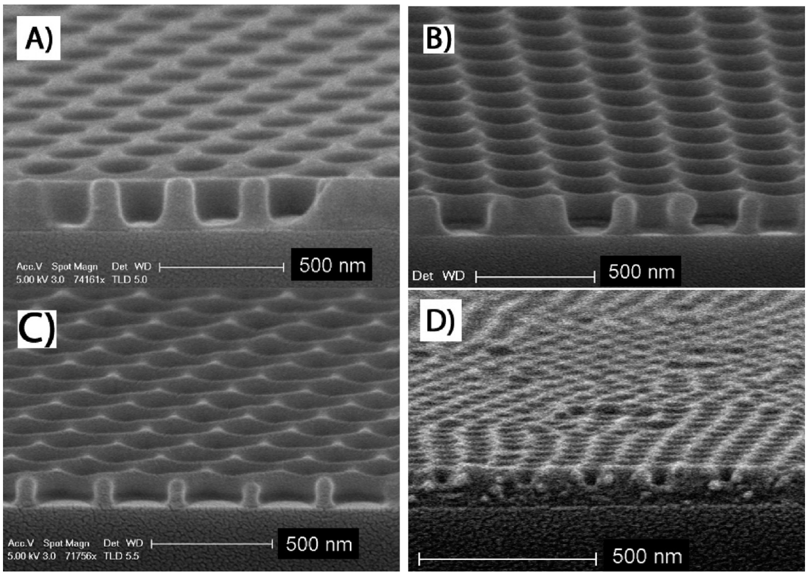

**Figure 10.** SEM images of (A) the thermoplastic resist NXR-1020 on silicon embossed with the stamp from Figure 8A; (B) the patterned film in B exposed to O$_2$ plasma for 30 s; (C) the patterned film in B exposed to O$_2$ plasma for 60 s; and (D) the thermoplastic resist embossed with the stamp from Figure 8C.

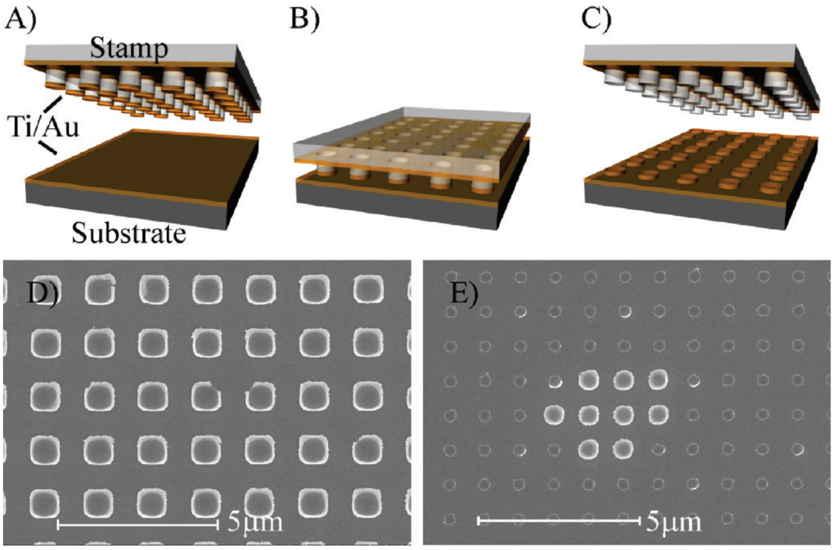

**Figure 11.** Top: Process for nanotransfer printing (nTP): (A) Ebeam evaporation of titanium and gold (2 nmTi/20 nmAu) bilayer onto a substrate (Si) and a patterned SB2-F stamp. (B) Put the substrate and the stamp into contact. (C) Peel the stamp. Bottom: SEM images of transferred pattern of gold with periodicity of 1.7 $\mu$m (D) and 1.1 $\mu$m (E).

the stamp bearing the sub-100 nm features. The successful pattern replication is evident in Figure 10D, without any distortions of the posts.[31]

**Nano-Transfer Printing.** Nanotransfer printing provides a simple and effective way to transfer submicrometer features from one substrate to another, thus increasing the repertoire of nanofabrication strategies.[32] Using the fluorinated stamp SB2-F, we employed the nanotransfer printing process for gold nanostructures as shown in Figure 11A−C. In this process, a blank silicon substrate (receiver) and the patterned SB2-F stamp were coated with titanium and gold bilayers (2 mm/20 nm). The thin layer of titanium acts as an adhesion layer for the top gold layer in both cases. The two gold surfaces were then put into contact, and the gold on the stamp relief patterns was transferred to the receiver through cold welding (Figure 11B). To facilitate conformal contact between the stamp and the receiver, a backing layer of $\sim$4 mm thick PDMS (Sylgard 184) was added to the SB2-F stamp. Figure 11d shows the SEM image of the transferred gold pads ($\sim$1 mm in diameter and $\sim$1.7 mm in periodicity) uniformly over a large area. However, the transfer process is less effective (partial transfer) for smaller size features ($\sim$0.6 $\mu$m in diameter and $\sim$1.1 $\mu$m in periodicity), as shown in Figure 11e, mostly due to the difficulty in obtaining conformal contact between the SB2-F and the receiver.

---

(31) We must note that the film thickness was approximately double the size of the posts due to the same processing conditions of the previous example, leading to a scum layer of similar height to the posts. The system can be further optimized by spin coating the resist to a thickness comparable to the height of the posts.

(32) Menard, E.; Bilhaut, L.; Zaumseil, J.; Rogers, J. A. *Langmuir* **2004**, *20*, 6871–6878.

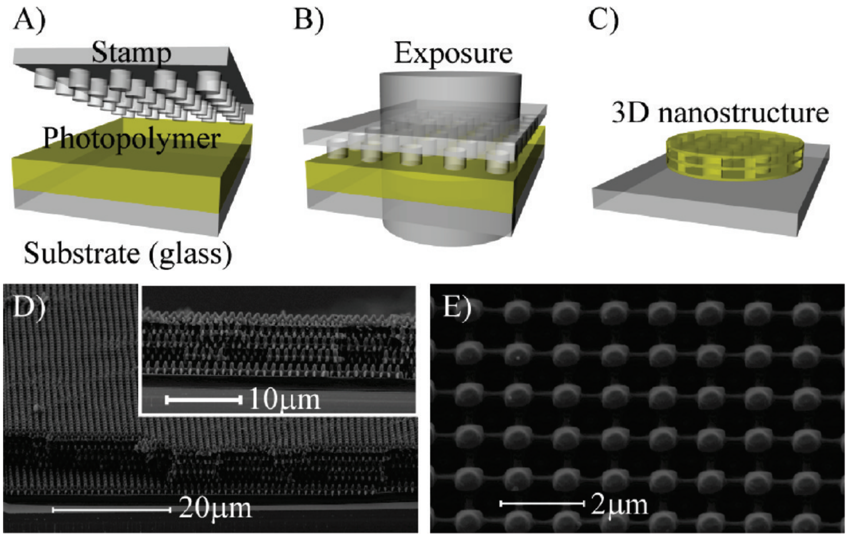

**Figure 12.** Top: Process for proximity-field patterning (PnP). (A) Spin coat a layer of photopolymer (SU8-10, ~10 $\mu$m) onto a glass substrate. (B) Bring the patterned SB2 phase mask into contact with the photopolymer and expose with a 800 nm light source. (C) Remove the phase mask, develop unexposed regions to yield 3D nanostructure. Bottom: SEM images of the 3D nanostructure in (D) tilted view together with cross-section (inset) and (E) top view.

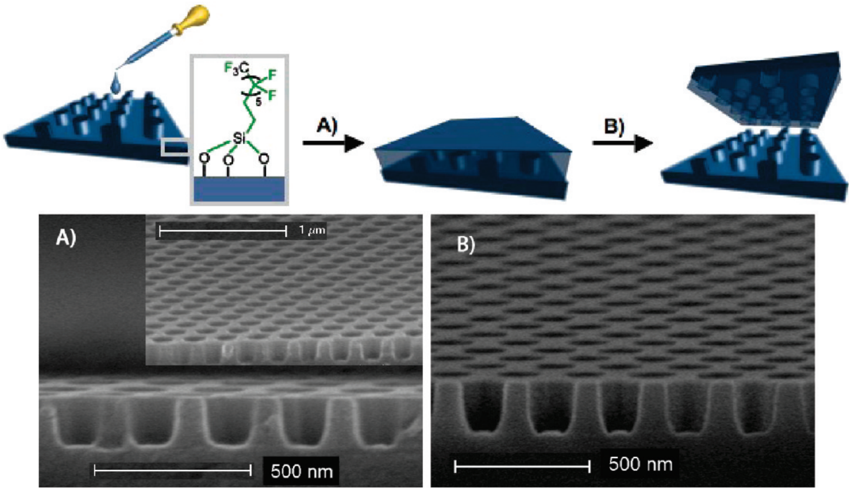

**Figure 13.** Top: Replica molding process with a fluorinated release layer in SB2-F. (B) cast thiol−ene mixture on top of SB2-F and photocure. (B) Peel off the SB2 stamp. Bottom: (A) SEM image of the SB2 replica of the master and (B) the patterned master silicon wafer.

**Proximity-Field Nanopatterning (PnP).** The ability of SB2 to replicate submicrometer features and its transparency in the visible range make it suitable for applications in phase mask lithography. Here, we demonstrate the use of SB2 as a phase mask to fabricate a 3D nanostructure through two-photon proximity-field nanopatterning (2ph-PnP).[33] The fabrication process is shown in Figure 12, top. The phase mask was generated from a photoresist pattern on $SiO_2$/Si substrate that consists of a square array of holes with diameter of ~0.66 $\mu$m, periodicity of ~1.1 $\mu$m, and relief depth of ~0.40 $\mu$m. Blank exposure with an 800 nm light source through the phase mask generates a 3D optical interference pattern in the photoactive polymer. The developing process removes the unexposed regions and creates a well-defined 3D nanostructure in the photopolymer layer. The SEM images in Figure 11D,E show the remarkably well-defined 3D nanostructure that was fabricated using the SB2 stamp.

**Polymeric Master Replicas.** An additional advantage of the surface treatment of the PMMS stamps is the ability to create replicas of the original master. Taking advantage of the polymeric replicas for further stamp fabrication minimizes damage to the hard master through wear-and-tear. Using the fluorinated stamp SB2-F, we employed the process highlighted in Figure 13, top. The same process for stamp fabrication described earlier was employed but using the polymeric stamp as the mold. After curing, the new polymeric replica mold composed of SB2 was easily peeled. This process highlights the fact that the surface treatment process left negligible amounts of thiol−ene functional groups capable of covalent attachment to the freshly cured SB2. In fact, peeling the replica was not possible without the surface treatment of

---

(33) Shir, D. J.; Jeon, S.; Liao, H.; Highland, M.; Cahill, D. G.; Su, M. F.; El-Kady, I. F.; Christodoulou, C. G.; Bogart, G. R.; Hamza, A. V.; Rogers, J. A. *J. Phys. Chem. B* **2007**, *111*, 12945–12958.

the patterned PMMS. The resulting SEM image of the polymeric replica of the master is shown in Figure 13A, bottom. The replicated pattern demonstrates that the high-fidelity features of the stamp containing posts are well replicated, and the polymeric replica accurately resembles the original master silicon mold shown in Figure 13B, bottom.

## Conclusions

In summary, this manuscript describes the successful pattern replication of resists through various techniques, reaching sub-100 nm resolution. The polymeric stamps employed are composed of inexpensive materials based on PMMS and organic cross-linkers that have a number of advantages when compared to traditional materials. Surface chemistry modifications lead to hydrophilic stamps that can be functionalized with a fluorinating agent to minimize adhesion. These materials are thermally stable up to approximately 225 °C, as characterized by TGA, do not undergo any phase transitions between −80 and 200 °C, and are optically clear and transparent above 300 nm. These characteristics, along with the outstanding mechanical properties, render the materials useful in numerous soft lithography applications. Furthermore, the facile surface chemistry modification, without the destruction of the nanopatterned structures, opens many options for further processing strategies.

## Experimental Section

**Materials.** Triallyl cyanurate (TAC) and 2,2-dimethoxy-2-phenylacetophenone (DMPA) were purchased from Aldrich. Tridecafluoro-1,1,2,2-tetrahydrooctyl)trichlorosilane (TDFOCS, SIT-8174.0) and poly[(mercapto-propyl)methylsiloxane] (PMMS, SMS-992) were purchased from Gelest. Ethoxylated (4) bisphenol A dimethacrylate (BPADMA) was kindly donated by Sartomer.

**Stamp Fabrication.** The stamps were fabricated as previously described.[7] Briefly, the sample blend with the composition in Scheme 1 was mixed in a microcentrifuge tube, including < 1% by weight of the photoinitiator. For example, 0.6 g of PMMS, 0.4 g of TAC, 0.1 g of BPADMA, and approximately 1 mg of DMPA were thoroughly mixed in a vortexer. The blend was then cast on top of the master, within the cavity between a spacer (typically 0.5 mm thick) and a glass plate. The sample was then photolyzed with a 365 nm wavelength lamp (intensity ca. 4.6 mW $cm^{-2}$) for 2 min through the face of the glass. The free-standing films were then peeled from the glass and the silicon master.

**Characterization.** UV−vis spectra were obtained using an Agilent Technologies spectrophotometer, model 8453. The mounted films were approximately 0.5 mm thick. Thermogravimetric analysis (TGA) and differential scanning calorimetry (DSC) were performed with analyzer models TGA-Q50 and DSC-Q10, respectively, from TA Instruments.

X-ray photoelectron spectroscopy (XPS) measurements were performed using an Axis Ultra XPS system (Kratos) with a monochromatic Al KR X-ray source (1486.6 eV) operating at 225 W under $7 \times 10^{-9}$ Torr vacuum. Charge compensation was carried out by injection of low-energy electrons into the magnetic lens of the electron spectrometer. The pass energy of the analyzer was set at 80 eV. The energy resolution was set at 0.1 eV with a dwell time of 100 ms. The spectra were analyzed using CasaXPS v. 2.3.12 software.

**Thin-Film Resist Preparation.** The resists employed for SSFIL and SNIL without the transfer layer were prepared by spin coating onto a silicon wafer a 3% solution of NXR-2010 (photoresist) or NXR 1020 (thermoplastic resist) at 4000 rpm for 45 s. The resists were imprinted using the automated Nanonex Imprinter NX 2000.

**Nano-Transfer Printing.** The stamp based on SB2 was fabricated with a pattern of photoresist on a $SiO_2$/Si substrate in a geometry of square arrays with holes having a diameter of ~1 μm, periodicity of ~1.7 μm, and a relief depth of ~0.4 μm. The patterned stamp was exposed to oxygen plasma (15 s) and TDFOCS vapor (30 min). The stamp and a blank silicon substrate were then coated with a double layer of titanium/gold (2 nm/20 nm) by e-beam evaporation. When the coated stamp and silicon substrate were put into contact (~5−10 min), cold welding of the gold layers enabled the transfer of gold from the relief regions on the stamp onto the silicon substrate.

**Two Photon Proximity-Field Nanopatterning (2ph-PnP).** The phase mask based on SB2 was cast onto a master with square arrays of holes (diameter ~ 0.66 μm, periodicity ~ 1.1 μm, relief depth ~ 0.40 μm) of photoresist on a $SiO_2$/Si substrate. The patterned phase mask was put into contact with a photopolymer layer (SU8-10, Microchem, ~10 μm) coated on a glass substrate. Blank exposure through the phase mask and photopolymer layer generated the 3D optical interference patterns that are recorded by the photopolymer layer, followed by removing the unexposed regions in a developing process to yield high quality 3D structures over large area. A light source with wavelength of 800 nm was used for the exposure.

**Master Mold Replicas.** The patterned stamps based on SB2 were exposed to oxygen plasma for 15 s (to yield SB2-OH). Then, SB2-OH was exposed to tridecafluoro-1,1,2,2-tetrahydrooctyl)trichlorosilane (TDFOCS) vapor for 20−30 min under reduced pressure. Finally, the thiol−ene blends were cast and cured on top of the fluorinated stamp (SB2-F). Peeling the sample yielded a stamp with the replica features of the original silicon master.

**Acknowledgment.** Financial support from the NSF (CHE-0514031 and the MRSEC Program DMR-0520415 [MRL-UCSB]), Mitsubishi Chemical Center for Advanced Materials (MC-CAM) and Mitsubishi Chemical Group Science and Technology Research Center, Inc., is gratefully acknowledged. Some of this work is supported by the U.S. Department of Energy, Division of Materials Sciences under Award No. DE-FG02-07ER46471, through the Materials Research Laboratory and Center for Microanalysis of Materials (DE-FG02-07ER46453) at the University of Illinois at Urbana-Champaign. L.M.C. also thanks the Regents of the University of California for a President's Fellowship.